Front. Earth Sci. 2019, 13(2): 336–350
https://doi.org/10.1007/s11707-018-0735-7

RESEARCH ARTICLE

Analysis of the relation between ocean internal wave parameters and ocean surface fluctuation

Yufei ZHANG (✉)[1], Bing DENG[2], Ming ZHANG[3]

1 National Marine Environmental Forecasting Center, Beijing 100081, China
2 Beijing Applied Meteorology Institute, Beijing 100029, China
3 PLA University of Science and Technology meteorological and Oceanographic Institute, Nanjing 211101, China

© Higher Education Press and Springer-Verlag GmbH Germany, part of Springer Nature 2018

Abstract The relation between ocean internal waves (IWs) and surface fluctuation is studied using a quasi-incompressible two-dimensional linear ocean wave model. The main conclusions are as follows: the IW parameters can be obtained by solving the boundary value problem of ordinary differential equations with the frequency, wave number, and amplitude of the surface fluctuation. When the ocean surface fluctuation state is given, the ocean IW presents a different structure, i.e., the uncertainty of the solution, which reflects the characteristics of the inverse problem. To obtain a definite solution, this study proposes constraint conditions for the inverse problem, namely, the relationship among background flow, buoyancy frequency, sea surface height, and geostrophic parameters. The necessary and sufficient conditions for the existence of IWs and external waves (surface wave) can be obtained according to the different constraint conditions. The amplitude of the surface fluctuation is positively correlated with IWs, and they share the same frequency and wave number. We also examined the relationship between the vertical structure, the maximum amplitude, and the constraint conditions. For a certain wave number, when the ocean environment is defined, the natural frequency (characteristic frequency) of IWs can be obtained. If the frequency of the surface fluctuation is similar or equal to the natural frequency, the resonance phenomenon will occur and can result in very strong IWs. The presented theory can serve as a basis for the analytical estimation of IWs.

Keywords constraint condition, surface fluctuation, internal wave, inverse problem

Received April 17, 2018; accepted September 3, 2018

E-mail: 15066836807@163.com

1 Introduction

Internal waves (IWs) are mesoscale phenomenon occurring internally in the ocean (Alpers, 1985; Feng, 1999). Stable density stratification in seawater is a requirement for the existence of IWs. The distribution of seawater and hydrologic features is complicated by the occurrence of IWs. Therefore, the dynamics of IWs (Xu, 1999; Fan, 2002) should not be ignored. The study of IWs is not only significant to the theoretical study of ocean dynamics but also to the safe exploitation of ocean resources (Zhang and Zhang, 2009; Muacho et al., 2014; Da Silva et al., 2015).

State-of-the-art *in-situ* methods to observe IWs include anchor array observations, dragging and throwing observations, neutral float observations, and acoustic observations. However, the data are limited by spatial coverage (Zong and Ou, 2011). The usage of space-borne cameras, visible and infrared scanners, and synthetic aperture radar (SAR) makes up the data shortage from *in-situ* measurements with large spatial coverage spanning thousands of square kilometers (Liu et al., 1998; Zong and Ou, 2011). However, remote sensing data cannot be used directly in the study of IWs, but *in-situ* data can. Satellite imagery captures ocean signals from the ocean surface but cannot reveal the vertical structure, maximum intensity, or various parameters of oceanic IWs directly. To observe features of IWs at the ocean surface, the first challenge is to determine the relationship between IWs and surface fluctuation.

Based on measured data from the Messina channel, the relationship between IWs and their surface signal detectable in remotely sensed images has been examined (Brandt et al., 1999). The results showed that the dynamics of IWs can be observed in radar imaging of the ocean surface. The interaction mechanism between the free surface and IWs in a two-layer fluid based on the potential flow theory of water waves shows that the coupling interaction between the surface wave mode and the IW mode must be taken

into account for cases with a large density difference between the two layers (Wei et al., 2003). A numerical flume with two layers has been used to simulate the propagation of IWs over various topographies and to investigate the development, propagation, and dissipation mechanisms of IWs (Chen et al., 2016). The results show that strong mixing and water exchange occur during IW propagation and result in intense convergence and dispersion, which lead to strong free surface flow and create noticeable free surface waves. The shapes of free surface waves and IWs have opposite direction. In addition, there is a close relationship between IWs and ocean surface waves. The resonant interactions of IWs and ocean surface waves have been analyzed as IWs pass over various types of sea floor surfaces. The results indicate that IWs and surface waves move in the same phase and that both wave types have the same wavelength. Various methods have been proposed to retrieve the seawater state parameters from SAR imagery according to the Korteweg–de Vries equations with the imaging mechanism of SAR under two-layer approximations, assuming that the density of the upper and the lower layers is different (Liu et al., 1998; Porter and Thompson, 1999; Li et al., 2000; Fan et al., 2010; Guo and Chen, 2014; Fan et al., 2015). The characteristics of IWs in the South China Sea have been previously discussed (Li, 2014; Alford et al., 2015; Xu et al., 2016; Yang et al., 2016). The results show that the vertical structure distribution of IWs cannot be extracted with the two-layer ocean model. The error can be significant when the difference indensity is not obvious (Zeng, 2002). However, the formation conditions of IWs is still not clear, which motivates us to develop a theoretical model to establish the relationship between IWs and sea surface fluctuations under a continuous stable stratified marine environment. This work proposes a model under continuous stable density stratification that solves boundary value problems of ordinary differential equations for the relation between IWs and surface fluctuation. The model can lead to an analytical solution under ideal conditions. We also discuss whether the surface fluctuation can be used to extract the continuous vertical distribution of parameters, such as the amplitude and intensity of IWs. How could the IWs relate to the characteristics of the ocean, such as background flow and buoyancy frequency? Is it possible for an IW to be strong but cause a small fluctuation on the surface? The present study provides ideas and the theoretical basis for the analytical estimation of IWs.

2 Mathematical model

Wave properties were studied using the Navier-Stokes equations (Deng and Zhang, 2006; Zhang et al., 2007; Yuan et al., 2011; Zhang et al., 2012; Deng et al., 2014, 2017), which are employed to reflect non-viscous, adiabatic, non-hydrostatic, and quasi-incompressible conditions. A term related to the earth's rotation is included in the equation. The vertical coordinate z is from the seafloor to the surface where $z = 0$ denotes the seafloor. The x-axis reflects the direction of wave propagation. The perturbation occurs in an ocean uniformly in the y direction, which means that $\frac{\partial}{\partial y} = 0$. Assuming that the atmospheric pressure is a constant, the two-dimensional non-hydrostatic linearization control equations are given as:

$$\begin{cases} \left(\frac{\partial}{\partial t} + \overline{u}\frac{\partial}{\partial x}\right)v + f\frac{\partial \psi}{\partial z} - \frac{\mathrm{d}\overline{v}}{\mathrm{d}z}\frac{\partial \psi}{\partial x} = 0 \\ \left(\frac{\partial}{\partial t} + \overline{u}\frac{\partial}{\partial x}\right)\tilde{\rho} + f\frac{\mathrm{d}\overline{v}}{\mathrm{d}z}\frac{\partial \psi}{\partial z} - f\frac{\mathrm{d}\overline{u}}{\mathrm{d}z}v - N_0^2\frac{\partial \psi}{\partial x} = 0 \\ \left(\frac{\partial}{\partial t} + \overline{u}\frac{\partial}{\partial x}\right)\nabla^2\psi - f\frac{\partial v}{\partial z} + \frac{\partial \tilde{\rho}}{\partial x} - \frac{\mathrm{d}^2\overline{u}}{\mathrm{d}z^2}\frac{\partial \psi}{\partial x} = 0 \end{cases}, \quad (1)$$

where t denotes time and $u \equiv \rho_0 u'$, $v \equiv \rho_0 v'$, $w \equiv \rho_0 w'$, and $\rho_0 \equiv -g\rho'$, where u',v',w' are the velocity perturbation components in the x, y, and z directions, respectively, and ρ' is the density perturbation. N_0 is the buoyancy frequency. The items $\overline{u}$, $\overline{v}$ are z-dependent components of the horizontal background flow in the x and y directions, respectively. Hence, $\frac{\mathrm{d}\overline{u}}{\mathrm{d}z}$ and $\frac{\mathrm{d}\overline{v}}{\mathrm{d}z}$ change with variable z. The velocity of an IW is the sum of the background flow ($\overline{u}$, $\overline{v}$, $\overline{w}$) and velocity perturbation components (u',v',w').

In Eq. (1), ρ_0 is the normalized density, g is the gravitational acceleration, f is the geostrophic parameter, ψ is the stream function, and $u \equiv \rho_0 u' = \partial\,\psi/\partial\, z$, $w \equiv \rho_0 w' = -\partial\,\psi/\partial\, x$, and $N_0^2(z) = -\frac{g}{\rho_0}\cdot\frac{\mathrm{d}\hat{\rho}(z)}{\mathrm{d}z} > 0$. $\hat{\rho}(z)$ is the typical value of the density distribution in the vertical direction. The 2-dimensional Laplace operator is given by $\nabla^2 = \frac{\partial^2}{\partial x^2} + \frac{\partial^2}{\partial y^2}$.

The present paper only considers the situation in which the background flow and the propagation of the IWs have the same direction, thus, $\overline{u} = \overline{u}(z)$, $\overline{v} = 0$. Eq. (1) can be simplified as follows:

$$\begin{cases} \left(\frac{\partial}{\partial t} + \overline{u}\frac{\partial}{\partial x}\right)v + f\frac{\partial \psi}{\partial z} = 0 \\ \left(\frac{\partial}{\partial t} + \overline{u}\frac{\partial}{\partial x}\right)\tilde{\rho} - f\frac{\mathrm{d}\overline{u}}{\mathrm{d}z}v - N_0^2\frac{\partial \psi}{\partial x} = 0 \\ \left(\frac{\partial}{\partial t} + \overline{u}\frac{\partial}{\partial x}\right)\nabla^2\psi - f\frac{\partial v}{\partial z} + \frac{\partial \tilde{\rho}}{\partial x} - \frac{\mathrm{d}^2\overline{u}}{\mathrm{d}z^2}\frac{\partial \psi}{\partial x} = 0 \end{cases}. \quad (2)$$

The lower boundary is considered a horizontal rigid boundary (like a horizontal seabed without any terrain). According to Fourier analysis, all waves can be resolved as a superposition of simple harmonic waves. Thus, assuming a simple harmonic wave on the sea surface that propagates along the x direction, the boundary conditions are:

$$z = 0,\ w = 0;\ z = H,\ w = W_H\cos(kx-\sigma t), \quad (3)$$

where W_H, k, and σ are the amplitude, the wave number of vertical movement, and the frequency of the ocean upper boundary, respectively. All parameters are set to a real constant and are greater than zero. H is the mean sea surface height, namely, the thickness between the upper boundary and the lower boundary of the sea. Using boundary conditions (Eq. (3)), the solution of Eq. (2) can be given by:

$$\begin{pmatrix} v \\ \tilde{\rho} \\ \psi \end{pmatrix} = \begin{pmatrix} V(z)\cos(kx-\sigma t) \\ P(z)\sin(kx-\sigma t) \\ \Psi(z)\sin(kx-\sigma t) \end{pmatrix}, \quad (4)$$

where $V(z)$, $P(z)$, $\Psi(z)$ are real functions. Their absolute values are the vertical amplitude of v, $\tilde{\rho}$, ψ. Let $\omega(z) = \sigma - \overline{u}(z)\cdot k$, then the following equations can be obtained:

$$\begin{cases} -\omega V - f\dfrac{\mathrm{d}\Psi}{\mathrm{d}z} = 0 \\ -\omega P - f\dfrac{\mathrm{d}\overline{u}}{\mathrm{d}z}V - kN_0^2\Psi = 0 \\ -\omega\left(\dfrac{\mathrm{d}^2\Psi}{\mathrm{d}z^2} - k^2\Psi\right) - f\dfrac{\mathrm{d}V}{\mathrm{d}z} + kP - k\dfrac{\mathrm{d}^2\overline{u}}{\mathrm{d}z^2}\Psi = 0 \end{cases}. \quad (5)$$

The boundary conditions are as follows:

$$z = 0,\ \partial\psi/\partial x = 0;$$

$$z = H,\ \partial\ \psi/\partial\ x = -W_H\cos(kx-\sigma t). \quad (6)$$

This means:

$$z = 0,\ \Psi = 0;\ z = H,\ \Psi = -W_H/k = \Psi_H.$$

In this case, Eq. (5) and boundary conditions (Eq. (6)) constitute a boundary value problem of the variable coefficient ordinary differential equations set.

Using $\overline{u}_z = \dfrac{\mathrm{d}\overline{u}}{\mathrm{d}z}$, $\overline{u}_{zz} = \dfrac{\mathrm{d}^2\overline{u}}{\mathrm{d}z^2}$, Eq. (5) without V, P can be written as:

$$\omega(\omega^2-f^2)\frac{\mathrm{d}^2\Psi}{\mathrm{d}z^2} - 2kf^2\overline{u}_z\frac{\mathrm{d}\Psi}{\mathrm{d}z} + \left[k^2\omega(N_0^2-\omega^2) + k\omega^2\overline{u}_{zz}\right]\Psi = 0. \quad (7)$$

In Eq. (7), the highest power of σ is 3 in $\dfrac{\mathrm{d}^2\Psi}{\mathrm{d}^2z}$, which corresponds to three waves in the eigen value problem of the equations set under homogeneous boundary conditions. Two of the waves are internal inertia gravity waves in the opposite direction, and the other is a vortex wave caused by the vertical shear of the background flow (Deng et al., 2014).

This work focuses on internal gravity waves (internal inertia gravity waves). The problem can be simplified by filtering the vortex wave through the approximation of the fast wave.

The approximation of the fast wave can be considered when $|\sigma| \gg |\overline{u}_z|$ or ignoring the rotation of the earth, i.e., when frequency σ is high (fast wave), the vertical shear of the background flow is not too large, or the system time scale is so small that the geostrophic effect is insignificant. The $2kf^2\overline{u}_z\mathrm{d}\Psi/\mathrm{d}z$ part in Eq. (7) is insignificant; therefore, the equation can be rewritten by fast wave approximation as:

$$(\omega^2-f^2)\frac{\mathrm{d}^2\Psi}{\mathrm{d}z^2} + \left[k^2(N_0^2-\omega^2) + k\omega\overline{u}_{zz}\right]\Psi = 0. \quad (8)$$

If the wave is observed near the equator or its time scale is less than 3 hours, the f in Eq. (8) can be ignored. Then, the equation can be simplified to the classic Taylor-Goldstein equation. The internal inertial gravity wave becomes an internal gravity wave. Here, IWs with a long period (12.5 h) are considered, and f is not ignored. Therefore, Eq. (8) includes the internal inertial gravity waves, which is developed based on the classic Taylor-Goldstein equation. The variable coefficient ordinary differential equation can be adapted as:

$$\frac{\mathrm{d}^2\Psi}{\mathrm{d}z^2} + \frac{k^2(N_0^2-\omega^2) + k\omega\overline{u}_{zz}}{\omega^2-f^2}\Psi = \frac{\mathrm{d}^2\Psi}{\mathrm{d}z^2} + Q(z)\Psi = 0. \quad (9)$$

In Eq. (9), if the background flow $\overline{u}$ or the buoyancy frequency N_0 is not constant, it is usually difficult to obtain an analytical solution and it may be unstable. Numerical methods have been used to study Eq. (9) (Deng et al., 2016). Assuming that $\overline{u}$ and N_0 are constant, which is consistent with the formation and persistence of IWs and stable stratification of the ocean (Zhang and Zhang, 2009) an analytical solution can be obtained. Therefore, ω is a constant and can be defined as $\omega = \sigma - \overline{u}\cdot k$. Only the case with $\overline{u}$ and N_0 being constant is discussed below. Thus, Eq. (9) can be simplified as follows:

$$\frac{\mathrm{d}^2\Psi}{\mathrm{d}z^2} + k^2\frac{N_0^2-\omega^2}{\omega^2-f^2}\Psi = 0. \quad (10)$$

Eq. (10) and boundary conditions (Eq. (6)) constitute a boundary problem of the second-order constant coefficient differential equation, which is simple to solve.

3 Analytical solution

To simplify the expression of Eq. (10), let $\eta = k \times \sqrt{|(N_0^2-\omega^2)/(\omega^2-f^2)|} > 0$ and ignore the situation $\omega = N_0$ and $\omega = f$. The analytical solution can be discussed in two different situations.

3.1 The first situation

In this situation, $k^2(N_0^2-\omega^2)/(\omega^2-f^2) > 0$. Eq. (10) can be rewritten as:

$$\frac{\mathrm{d}^2\Psi}{\mathrm{d}z^2} + \eta^2\Psi = 0. \tag{11}$$

Its general solution is as follows:

$$\Psi = A\cos(\eta z) + B\sin(\eta z). \tag{12}$$

According to boundary conditions (Eq. (6)), $A = 0$ and $B = \Psi_H/\sin(\eta H)$. Thus, the solution of Eq. (11) under boundary conditions (Eq. (6)) is:

$$\Psi(z) = \frac{\Psi_H}{\sin(\eta H)}\sin(\eta z) = -\frac{W_H}{k\sin(\eta H)}\sin(\eta z). \tag{13}$$

In Eq. (13), the vertical structure of Ψ is a sine function. η is the vertical wave number. Larger η values denote that the vertical structure is more complex.

As shown in Eq. (13), the Ψ depends on W_H/k, $\sin(\eta z)$ and $\sin(\eta H)$. The maximum value (Ψ_M) of Ψ can be estimated from Eq. (13):

$$\Psi_M = \max\left|\frac{W_H\sin(\eta z)}{k\sin(\eta H)}\right| \leqslant \frac{W_H}{k|\sin(\eta H)|}. \tag{14}$$

W_H/k is only determined by the sea surface fluctuation, i.e., the upper boundary conditions. The item $\sin(\eta z)$ defines the vertical structure of IWs. Because $|\sin(\eta H)| \leqslant 1$, the amplitude of the wave inside the sea is greater than or equal to its amplitude at a water depth H. Therefore, the wave is an IW. The vertical structure term $\sin(\eta H)$ is closely related to the marine environment. In addition to the wave number k and the frequency (ω) of the surface fluctuation, other factors that define the maximum of $|\Psi(z)|$ include the marine environmental factors N_0, $\overline{u}$, f, and H. When $\eta H \to l\pi$ (l is a positive integer), $|\sin(\eta H)| \to 0$ and $\Psi_M \to \infty$. Once the combination of these factors makes $|\sin(\eta H)| \to 0$, a greater amplitude of the IW will form and should be highly noticeable.

The vertical structure of IWs is defined by η. The extreme point of $|\Psi|$ is determined by $\sin(\eta z) = 1$ from the lower to the upper boundary when $H \geqslant (1/2)\pi/\eta$. $z = (l-1/2)\pi/\eta < H$, $l = 1,2,3,\ldots,\hat{l}$, where l is called the modal number of the IW. The value of the first extreme point of $|\psi|$ is $\dfrac{\pi}{2\eta}$, the second is $\dfrac{3\pi}{2\eta}$, and the rest can be assessed in the same manner until $(\hat{l}+1/2)\pi < \eta H$. The maximum mode is $\hat{l}$. There is a zero point between the two extreme points. The larger the $\hat{l}$ is, the more extreme and zero points there are. The maximum value of $|\psi|$ is $\dfrac{|\psi|}{|\sin(\eta H)|}$. The greater the number of extreme points and the higher the mode of the IW, the more complicated the vertical structure of the IW can be.

However, when $H < \pi/2\eta$, e.g., H is too small or η is too large, the Ψ is zero in the lower boundary. The $\sin(\eta H)$ can increase until it reaches the first extreme point. Hence, $|\Psi|$ reaches its maximum $|\Psi_H|$ at H when z reaches the upper boundary before the first extreme point. The wave is still an IW, and its mode is zero. The maximum of $|\Psi|$ appears at the upper boundary.

In the first situation when the IW appears, it can be inferred from

$$k^2(N_0^2-\omega^2)/(\omega^2-f^2) > 0,$$

where the conditions are $\{\omega | f < \omega < N_0|\} = (f, N_0)$. This is a necessary and sufficient condition for the formation of IWs. Although there is no wave at the height of H, which means that $z = H$, $w = 0$ with the rigid boundary approximation on the upper boundary, IWs still exist inside the sea. In this situation, the problem shifts from a boundary problem to an eigen value problem (Deng and Zhang, 2006).

3.2 The second situation

In the second case, $k^2(N_0^2-\omega^2)/(\omega^2-f^2) < 0$. Eq. (11) can be written as

$$\frac{\mathrm{d}^2\Psi}{\mathrm{d}z^2} - \eta^2\Psi = 0. \tag{15}$$

Its general solution is as follows:

$$\Psi = A\cosh(\eta z) + B\sinh(\eta z). \tag{16}$$

According to boundary conditions (Eq. (6)), $A = 0$ and $B = \Psi_H/\sinh(\eta H)$. Thus, the solution of Eq. (15) under boundary condition (Eq. (6)) is:

$$\Psi(z) = \frac{\Psi_H}{\sinh(\eta H)}\sinh(\eta z) = -\frac{W_H}{k\sinh(\eta H)}\sinh(\eta z). \tag{17}$$

In Eq. (17), $\sinh(\eta H) > \sinh(\eta z)$ in $(0, H)$. Hence, $\Psi(z) < \Psi_H$. The wave has its maximum amplitude at the sea surface. In addition, there is no zero point of the wave under the surface. The character of this wave corresponds with an external gravity inertial wave. The amplitude $|\Psi(z)|$, which is maximal on the ocean surface, decreases in a hyperbolic sine function into the seabed.

In short, for $k^2(N_0^2-\omega^2)/(\omega^2-f^2) < 0$, the requirement for the appearance of the external wave (surface wave) is that ω should fall outside of the closed interval between f

Table 1 The settings of the parameters in six typical cases

Case	N_0/s^{-1}	$\overline{u}$ /(m·s^{-1})	H/m
1	2.0×10^{-4}	0	460
2	2.0×10^{-4}	0.05	460
3	3.0×10^{-4}	0	460
4	3.0×10^{-4}	0.05	460
5	2.0×10^{-4}	0	200
6	1.0×10^{-4}	0	460

and N_0. In this situation, when there is no wave for the rigid boundary approximation at the height of H, the eigen value problem has only a zero solution, which shows that there is no wave inside the sea.

3.3 The expression of the wave parameters

After solving the equation of $\Psi(z)$ in the two situations above, the expressions of $V(z)$, $P(z)$ can be easily concluded: ω, $\overline{u}$ are constant, and $\mathrm{d}\overline{u}/\mathrm{d}z$ and $\mathrm{d}^2\overline{u}/\mathrm{d}z^2$ in the expression disappear. After getting $\Psi(z)$, $V(z)$, $P(z)$, the solution of v, $\tilde{\rho}$, ψ can be concluded from Eq. (4), which satisfies Eq. (2) and the boundary conditions (Eq. (3)). The solution of u,w can be resolved from $u=\partial\psi/\partial z$, $w=-\partial\psi/\partial x$.

The equations of the solutions of IWs are as follows:

$$\psi(x,z) = -\frac{W_H}{k\sin(\eta H)}\sin(\eta z)\sin(kx-\sigma t), \tag{18-1}$$

$$v = \frac{f\eta}{\omega}\frac{W_H}{k\sin(\eta H)}\cos(\eta z)\cos(kx-\sigma t), \tag{18-2}$$

$$\tilde{\rho} = \frac{kN_0^2}{\omega}\frac{W_H}{k\sin(\eta H)}\sin(\eta z)\sin(kx-\sigma t), \tag{18-3}$$

$$u = -\eta\frac{W_H}{k\sin(\eta H)}\cos(\eta z)\sin(kx-\sigma t), \tag{18-4}$$

$$w = \frac{W_H}{\sin(\eta H)}\sin(\eta z)\cos(kx-\sigma t). \tag{18-5}$$

The equations of the solutions of external waves are as follows:

$$\psi(x,z) = -\frac{W_H}{k\sin(\eta H)}\sinh(\eta z)\sin(kx-\sigma t), \tag{19-1}$$

$$v = \frac{f\eta}{\omega}\frac{W_H}{k\sin(\eta H)}\cosh(\eta z)\cos(kx-\sigma t), \tag{19-2}$$

$$\tilde{\rho} = \frac{kN_0^2}{\omega}\frac{W_H}{k\sin(\eta H)}\sinh(\eta z)\sin(kx-\sigma t), \tag{19-3}$$

$$u = -\eta\frac{W_H}{k\sin(\eta H)}\cosh(\eta z)\sin(kx-\sigma t), \tag{19-4}$$

$$w = \frac{W_H}{\sin(\eta H)}\sinh(\eta z)\cos(kx-\sigma t). \tag{19-5}$$

After getting v, $\tilde{\rho}$, ψ, u, w and by using the equations $(u', v', w')^{\mathrm{T}} = (u,v,w)^{\mathrm{T}}/\rho_0$ and $\rho' = -\tilde{\rho}/g$, the velocity disturbance field u', v', w', and the density disturbance field ρ' can be obtained. The stream function disturbance is $\psi' = \psi/\rho_0$. The above equations do not superimpose a constant background flow $\overline{u}$. When the item $\overline{u}$ is superimposed, the velocity in the x direction is $\overline{u}+u'$, while v', w' remains unchanged. The stream function is $\overline{u}z+\psi'$ with background flow added.

4 The case analysis

Six typical cases for visually expressing the configuration and the relationship between surface fluctuations and IWs are analyzed in the following. Among those cases, the parameters that refer to the marine environmental characteristics of IWs in the China Sea (Zhang and Zhang, 2009) are $L=1000$ m, $f=5\times10^{-5}$ s^{-1}, $T=12.5$ h, and $W_H=0.5$ cm/s. The analysis uses different buoyancy frequencies N_0, water depth H, and constant background flow $\overline{u}$. The settings of the various parameters are shown in Table 1. For each case, the patterns of ψ', $\Psi(z)$, w', and u' are shown in Figs. 1(a)–1(d), respectively. In the figures, the z-axis denotes the water depth, and the x-axis is the horizontal distance, except for Fig. 1(b), which shows the amplitude. Figure 1(a) shows the distribution of ψ', w', and u' when $t=0$, and Fig. 1(b) shows the distribution of $\Psi(z)$.

4.1 Case 1

Take the case where buoyancy frequency $N_0=2\times10^{-4}$ s^{-1} and the effect of the background is neglected flow, which means $\overline{u}=0$. The given parameters can generate IWs, i.e., $k^2(N_0^2-\omega^2)/(\omega^2-f^2)>0$.The wavelength of the stream function ψ' is the same as the surface fluctuation (Fig. 1). There is only one single loop in the vertical direction, and the circulation center is located at a height of 228 m from the lower boundary (Fig. 1(a)). The amplitude distribution of $\Psi(z)$ has only one extreme value in the whole body of water. The position of this extreme value is situated at the center of the stream function (Fig. 1(b)). The vertical motion of w' also shows a single loop, with a maximum of w' exceeding 15 cm/s at a height of 228 m (Fig. 1(c)). The amplitude of the loop is 30 times greater than that at the upper boundary.

The distribution of the field u' is different from the stream function Ψ and the vertical velocity w', where u' is

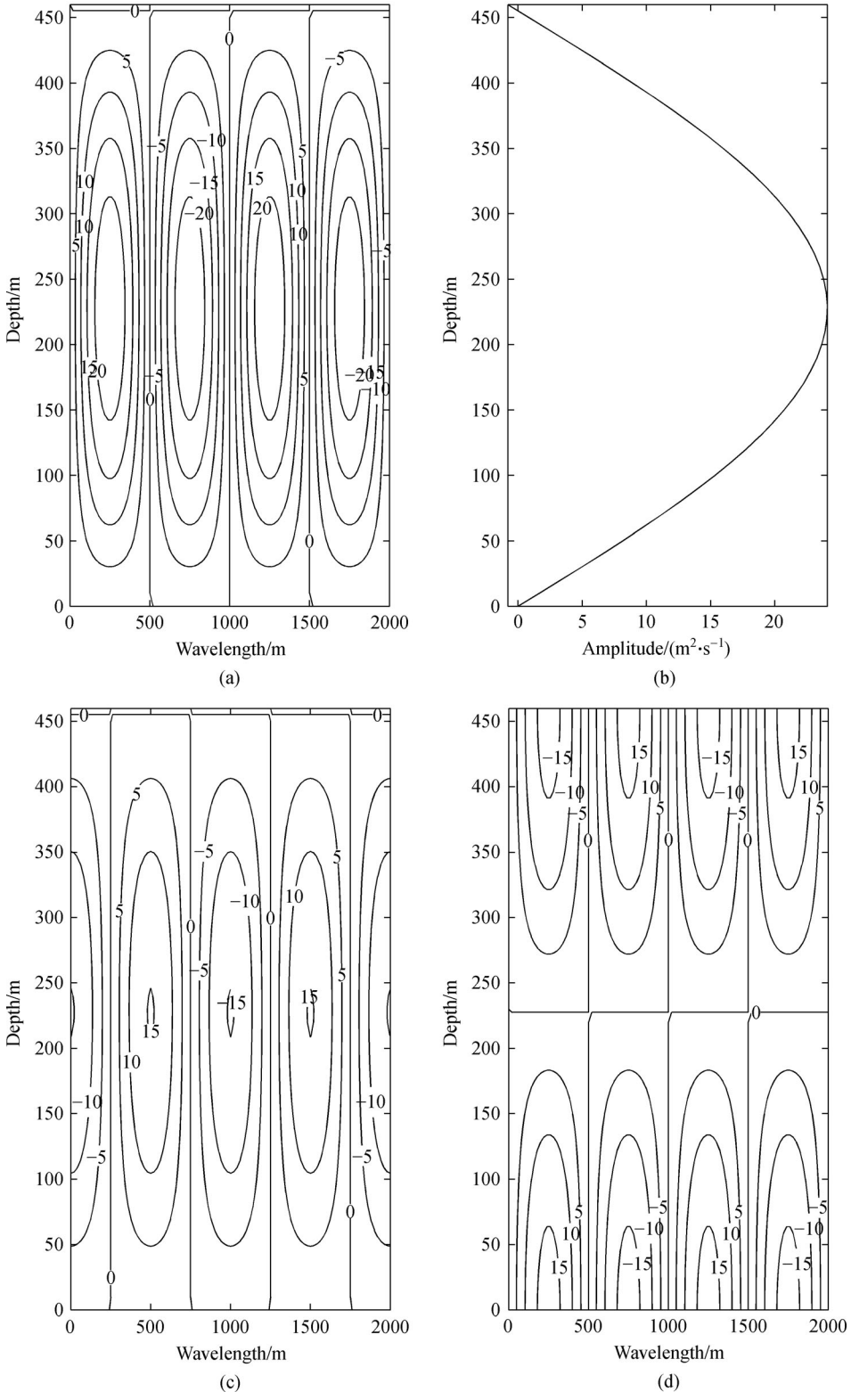

Fig. 1 The distribution of IW parameters in the first case. (a) The distribution of stream function; (b) $\Psi(z)$ distribution; (c) w' distribution; (d) u' distribution.

0 at the maximum of w'. Its maximum (>15 cm/s) is present in the upper and lower borders (Fig. 1(d)), and the direction of the upper and lower streams is opposite. The ocean wave is the same as the upper boundary fluctuation, and there is no phase change.

4.2 Case 2

In this case, the marine environment is the same as that in the first case except for the background flow $\overline{u} = 0.05$ m/s and still meets IWs existence conditions. The stream function contains the background flow, as shown in Fig. 2(a). $(\overline{u}z + \Psi)$, and is obviously different from the stream function in the first case. The single-loop current from the first case is replaced by the wave distribution. Its maximum appears at the height of 423 m, where the vertical amplitude of the streamline is approximately 25 m (Fig. 2(a)). The distribution of the $\Psi(z)$ (vertical amplitude) also has only one maximum value in the whole body of water, which appears at the height of 423 m, near the upper boundary (Fig. 2(b)).

In Fig. 2(c), the maximum vertical amplitude of the field w' also appears at the height of 423 m, which is much smaller than the corresponding value in the first case, e.g., approximately 0.55 cm/s. The distribution of the field is also significantly different from that of the first case. The large value of u' is mainly observed at the bottom of the water body. The velocity field near the upper boundary is very small and reaches 0 at 423 m (Fig. 2(d)). Compared with Case 1, the intensity of the IW is weakened due to the existence of background flow, and the position of the maximum vertical amplitude of the IW is raised upwards.

4.3 Case 3

To discuss the effect of the floating frequency, this case is set up similar to the first case, except for $N_0 = 3.0\times10^{-4}$ s^{-1}. It meets the IWs existence conditions. The stream function appears as a positive and negative two-circulation ring in the vertical direction. The central positions are situated at heights of approximately 130 m and 370 m (Fig. 3(a)). $\Psi(z)$ has a zero value and two extremes in the whole body of water. The position of the extreme point is consistent with the center of the stream function (Fig. 3(b)). The characteristics of the distribution of the vertical velocity w' are similar to the stream function, e.g., two-circulation distributions. The center position of w' is the same as the center position of the stream function, and the velocities of negative and positive circulation centers are approximately 1 cm/s and 0.5 cm/s, respectively (Fig. 3(c)). The distribution of the u' field (Fig. 3(d)) is different from the stream function and the vertical velocity, as a single loop is present between the vertical height of 125 m and 375 m, which is close to the center of the circulation, where the velocity is approximately 2.5 cm/s. The upper and lower boundaries have a half-circle circulation of the same phase.

4.4 Case 4

Case 4 is similar to Case 2, except that the floating frequency is set to $N_0 = 3\times10^{-4}$ s^{-1}. The case also meets the IW existence conditions. In this case, the distribution of the stream function is similar to that of Case 2, which is a simple harmonic shape (Fig. 4(a)). However, the phases of the upper and lower stream functions are opposite. The maximum vertical amplitude of the streamline appears at approximately 170 m (Fig. 4(b)). Compared with Case 2, the distribution of the extreme $\Psi(z)$ is shifted downward from the upper layer. The maximum intensities of w' and u' are approximately 0.5 cm/s (Fig. 4(c)) and 0.8 cm/s (Fig. 4(d)), respectively. The vertical motion in this case (w') shows one and a half loops, which is different from Cases 2 and 3. It can be concluded that the background flow and the floating frequency not only have a significant effect on the intensity of the IW but also its vertical structure and shape of motion.

4.5 Case 5

To study the effect of water depth on the IW, the other environmental parameters are the same as in Case 1 except that the water depth is 200 m. This case also meets the IW generation conditions. The stream function in the vertical direction only has half circulation, and a large area appears in the vicinity of the surface (Fig. 5(a)). The extreme point of $\Psi(z)$ appears at the upper boundary (Fig. 5(b)). The maximum value of w' is also located at the upper boundary, which is only 0.5 cm/s (Fig. 5(c)). The maximum value u' is observed at the lower boundary, which is approximately 0.5 cm/s, and the value is much smaller than the corresponding value of Case 1 (Fig. 5(d)).

4.6 Case 6

When the buoyancy frequency is set to $N_0 = 1.0\times10^{-4}$ s^{-1}, and the other marine environmental conditions remain the same as in Case 1, i.e., $k^2(N_0^2-\omega^2)/(\omega^2-f^2) < 0$, the case does not meet the conditions required for the generation of an IW. Therefore, this case only results in an external wave (surface wave). As shown in Figs. 6(a)–6(d), the largest amplitude of the stream function Ψ, the velocity u' and the vertical motion w' occur at the upper boundary and decrease as the depth increases. This is clearly different from the vertical structure of an IW.

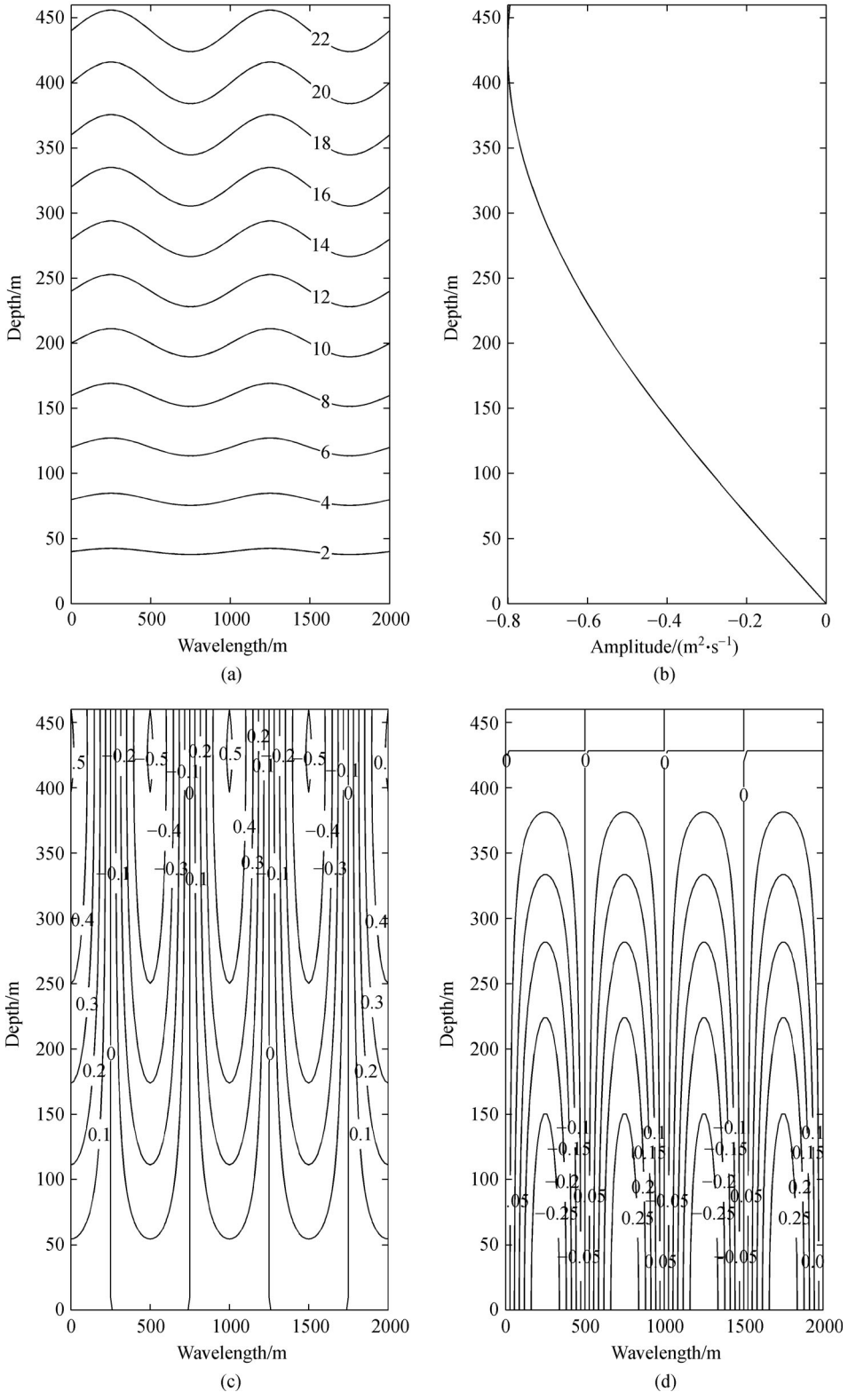

Fig. 2 The distribution of IW parameters in the second case. (a) The distribution of stream function; (b) $\Psi(z)$ distribution; (c) w' distribution; (d) u' distribution.

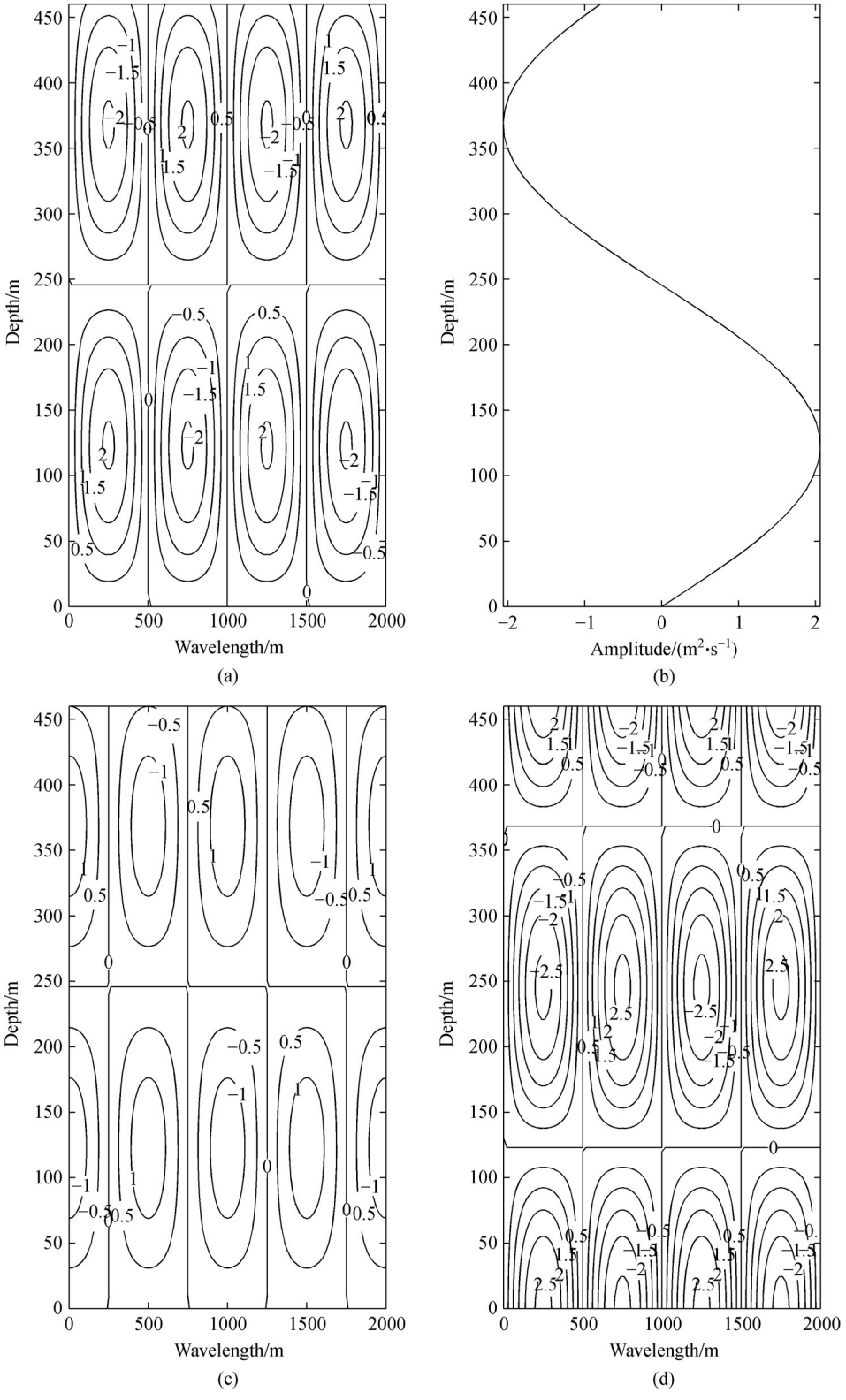

Fig. 3 The distribution of IW parameters in the third case. (a) The distribution of stream function; (b) $\Psi(z)$ distribution; (c) w' distribution; (d) u' distribution.

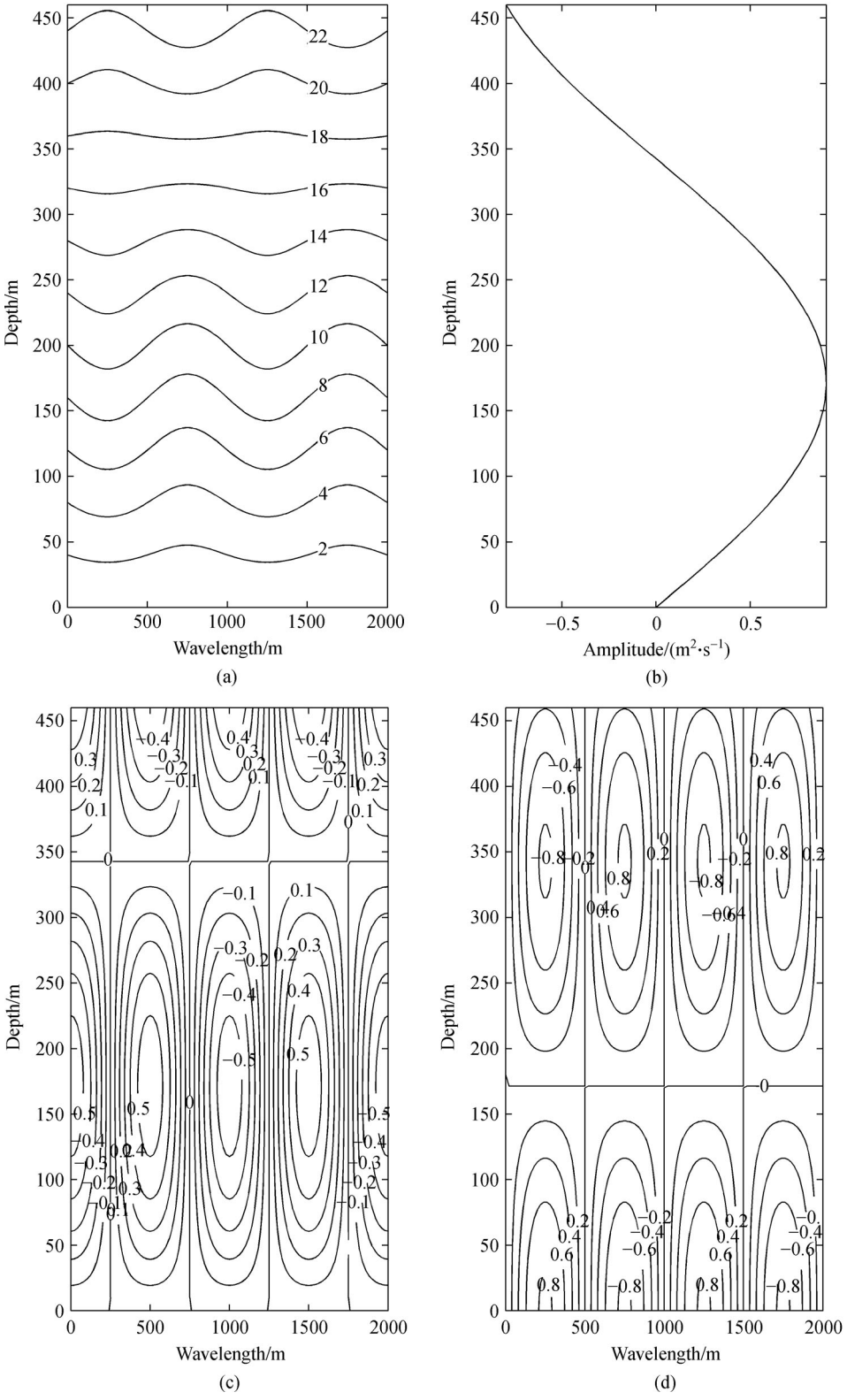

Fig. 4 The distribution of IW parameters in the fourth case. (a) The distribution of stream function; (b) $\Psi(z)$ distribution; (c) w' distribution; (d) u' distribution.

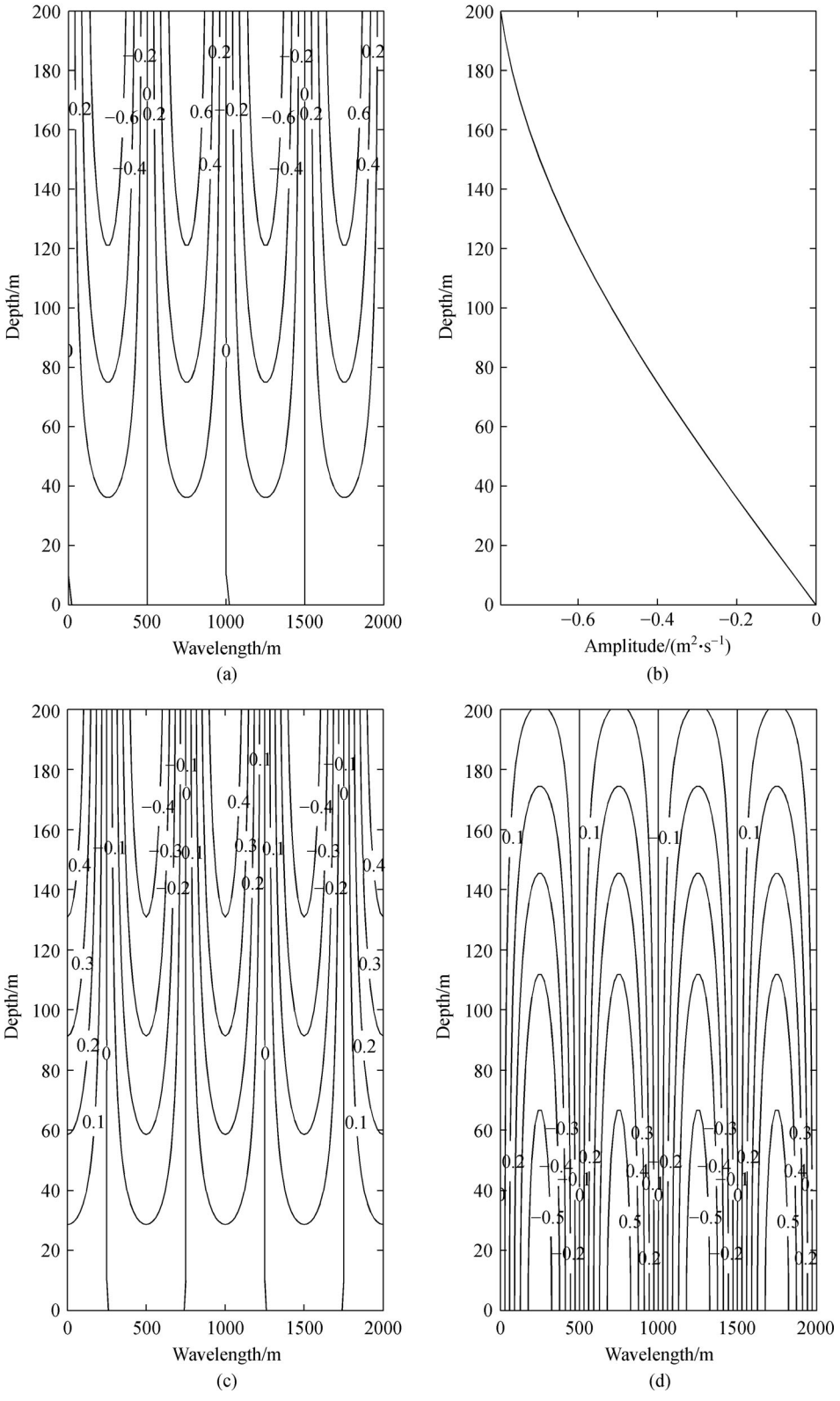

Fig. 5 The distribution character of IW in the fifth case. (a) The distribution of stream function; (b) $\Psi(z)$ distribution; (c) w' distribution; (d) u' distribution.

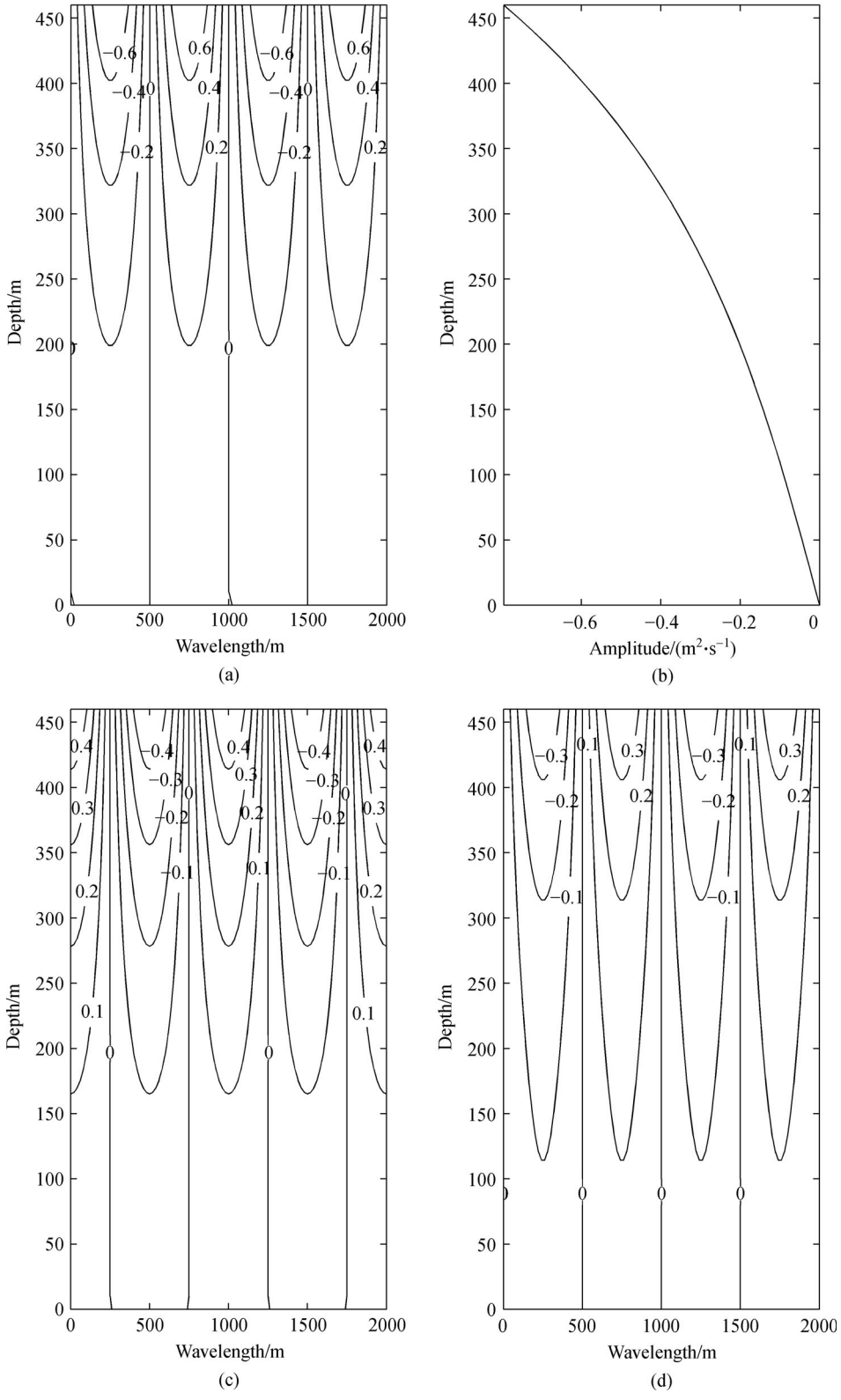

Fig. 6 The distribution character of the surface wave in the sixth case. (a) The distribution of stream function; (b) $\Psi(z)$ distribution; (c) w' distribution; (d) u' distribution.

5 Discussion

5.1 The constraint condition

According to the above results, different constraint conditions lead to completely different IW dynamics. The waves themselves also show different states with uncertain solutions, which also shows the characteristics of the inverse problem. To obtain a definite solution to the inverse problem, the constraint conditions must be given. The background state parameters of the ocean, i.e., background flow, buoyancy frequency, sea surface height, and geostrophic parameters are the constraint factors. Once the constraint conditions are defined, the solutions are also defined.

In the first situation, $k^2(N_0^2-\omega^2)/(\omega^2-f^2)>0$, which meets the IW existence conditions, and IWs are present in the vertical structure of the ocean. Under the constraint conditions, the amplitude of the stream function and the vertical velocity may reach their maximum within the ocean (e.g., Case 1). In the second situation, $k^2(N_0^2-\omega^2)/(\omega^2-f^2)<0$, the waves are external waves (surface waves). The maxima of the stream function and the vertical velocity are both at the sea surface. From the solutions, we can see that the vertical structure of internal and external waves is completely different. The IWs are consistent sine or cosine waves, while the external waves are hyperbolic sine or cosine waves that decay with the ocean depth.

Buoyancy frequency and background flow are two important constraint factors in this inverse problem. They define natural characteristics of the wave. Section 2 explains that the necessary and sufficient conditions for the existence of an IW is $\omega^2 \in (f^2, N_0^2)$. However, the necessary and sufficient condition for the existence of an external wave is $\omega^2 \notin (f^2, N_0^2)$. Because $\omega=\sigma-\overline{u}\cdot k$, the σ and k are estimated from the surface fluctuation. Therefore, the key constraint factors on the wave are the buoyant frequency N_0 and the background flow $\overline{u}$. The existence of background flow has a great impact on the results; although the background flow itself is a constant, the nature of the wave differs. The existence of the background flow changes ω ($\omega=\sigma-\overline{u}\cdot k$), which has the same frequency σ. The ω is the only factor in Eq. (10) that defines the character and shape of the wave when f and N_0 have not changed. Due to the existence of $\overline{u}$, ω is the frequency that influences the frequency σ through the Doppler shift. One should pay attention to the effect of background flow.

5.2 The resonance

When the upper boundary is just a wall, the boundary conditions are $z=0$, $\Psi=0$, $z=H$, $\Psi=0$. Solving the boundary problem of Eq. (10) converts it into an eigenvalue problem. The eigenvalue problem has non-zero solutions, and its characteristic frequency (Deng and Zhang, 2006) is

$$\tilde{\sigma}=\tilde{k}\overline{u}\pm\sqrt{\frac{\tilde{k}^2N_0^2H^2+n^2\pi^2f^2}{\tilde{k}^2H^2+n^2\pi^2}},$$

$$n=1,\ 2,\ 3,..., \tag{20}$$

where $\tilde{\sigma}$ and $\tilde{k}$ are the characteristic frequency and wave number when the mode is n, respectively. The modal eigen function expression is as follows:

$$\Psi(z)=C\sin\left(\frac{n\pi}{H}z\right)=C\sin(\tilde{\eta}z), \tag{21}$$

where C is a constant, which is the amplitude of the characteristic waves.

$$\text{Also, } \tilde{\eta}=n\pi/H=\tilde{k}\sqrt{\left(N_0^2-\tilde{\omega}^2\right)/(\tilde{\omega}^2-f^2)},$$

where $\tilde{\omega}=\tilde{\sigma}-\tilde{k}\cdot\overline{u}$.

When the background field and the environment are defined, i.e., N_0, $\overline{u}$, H, f are defined, and if there is a characteristic wave in a mode with the frequency $\tilde{k}$, the characteristic frequency $\tilde{\sigma}$ can be defined by Eq. (20). When $\tilde{\eta}=n\pi/H$, $\sin(\tilde{\eta}H)=0$. This is the upper boundary condition of the eigen value problem.

For the same ocean environment as the above eigen value problem, it has the same N_0, $\overline{u}$, H, and f. Eq. (10) and the boundary conditions (Eq. (6)) constitute a boundary value problem of partial differential equations.

In the first situation of Section 2, if $\sigma\to\tilde{\sigma}$ and $k\to\tilde{k}$ at the sea surface ($z=H$), $\eta\to\tilde{\eta}$. Since $\sin(\tilde{\eta}H)=0$, $\sin(\eta H)\to 0$. In Eq. (13), the vertical amplitude $\Psi(z)$ of the IWs is calculated from the surface wave, the denominator is $\sin(\eta H)$. If the denominator tends to 0, the maximum vertical amplitude of the IWs (Ψ_M) will be very large even if the amplitude of the surface wave W_H is small (see Case 1). Of course, when $\sin(\eta H)\to 0$, the amplitude of the IW in the actual ocean would not be infinite due to the viscosity and nonlinear characteristics of seawater.

When the frequency of the surface wave is similar to or equal to the natural frequency, the resonance phenomenon occurs.

However, no resonance phenomenon occurs in the second situation in the external wave because the eigen value problem has no non-zero solution. This is an important difference between the internal wave and the external wave.

5.3 Analytical estimation

With $u=-\dfrac{\eta W_H}{k\sin(\eta H)}\cos(\eta z)\sin(kx-\sigma t)$ and $u=\partial\psi/\partial z$, the following equation can be derived:

$$u = U(z)\sin(kx-\sigma t)$$
$$= -\frac{W_H}{k\sin(\eta H)}\eta\cos(\eta z)\sin(kx-\sigma t), \quad (22)$$

where $U(z)$ is the vertical structure of u,

$$U(z) = -\frac{\eta W_H}{k\sin(\eta H)}\cos(\eta z), \quad (23)$$

when $z = H$,

$$\frac{k}{\eta} = -\frac{W_H}{U_H}\cot(\eta H), \quad (24)$$

where U_H denotes the amplitude of u for the sea surface fluctuation. By the equation above, when the ocean parameters k, η, and H are given, W_H can be obtained by U_H, and vice versa.

The ratio of the wave number (k) to the vertical wave number (η) is subject to the constraint of Eq. (24). If the wave number (k), U_H, W_H, and the sea surface height H are given, the value η can be obtained by iteratively solving Eq. (24). When η is obtained, the vertical amplitude $W(z)$ equation can be solved by Eq. (18-5).

$$W(z) = W_H\frac{\sin(\eta z)}{\sin(\eta H)}. \quad (26)$$

If the U_H, W_H, and H are known, we can obtain the maximum vertical amplitude of the IW and its depth without σ and ω. This result is sure to receive more attention for marine safety applications.

If the ω, k, and f of the sea surface ($z = H$) are known, the stratification parameters of the ocean through the relationship $\eta^2 = k^2(N_0^2-\omega^2)/(\omega^2-f^2) > 0$ can be obtained by:

$$N_0^2 = \frac{\eta^2}{k^2}(\omega^2-f^2) + \omega^2. \quad (27)$$

6 Conclusions

This paper studies the relation between IW parameters and surface fluctuation using a quasi-incompressible non-hydrostatic two-dimensional linear ocean wave model. The main conclusions are as follows:

1) IW features can be obtained by solving the boundary value problem of an ordinary differential equation based on the frequency σ, the wave number k, and the amplitude of ocean surface fluctuation. When the background flow and the buoyancy frequency are both constant, an analytical solution can be obtained.

2) When the surface fluctuation state is given, the IW features present different shapes, which reflect the uncertainty of the solution. The uncertainty reflects the characteristics of the inverse problem. To obtain a definite solution, the constraint conditions of the inverse problem, such as the background flow, buoyancy frequency, sea surface height, and geostrophic parameters are imposed.

3) Depending on the different constraint conditions, the results can be divided into two completely different situations. One is the IW situation. In this situation, the necessary and sufficient conditions for wave formation are $\omega^2 \in (f^2, N_0^2)$. The other case is the external wave (surface wave) situation, in which the necessary and sufficient conditions for wave formation are $\omega^2 \notin [f^2, N_0^2]$.

4) The frequency and wave number of the IW are the same as the surface fluctuation. The greater the amplitude of the surface fluctuation is, the greater the amplitude of the IW is. They are positively correlated. Their amplitude is also related to $\sin(\eta H)$. The smaller $\sin(\eta H)$ is, the greater the amplitude is. However, it is possible that the amplitude of the IW is huge while the surface fluctuation is small. The vertical structure of the IW is related to the η. The greater the η is, the more complex the vertical structure is.

5) For a certain mode, once the ocean environmental factors are determined, the natural frequency (characteristic frequency) of the IW is also revealed. When the frequency and the wave number of surface waves are similar or equal to the natural frequency and the natural wave number, respectively, the resonance phenomenon occurs, and there can be very strong IWs. When this occurs, great attention must be paid to ensure marine safety is maintained.

In the case of the simplified stratification structure of the ocean, N_0 can be taken as a constant, but often there is a pycnocline in the actual ocean. Hence, N_0 cannot be constant. N_0 is a function of z. When N_0 is a function of z, $Q = [k^2(N_0^2(z)-\omega^2)]/(\omega^2-f^2)$ is a function of z as well. If $Q(z) > 0$ and $Q(z) \in [0,H]$, the conditions for the existence of IWs will be satisfied, i.e., $(N_0^2(z)-\omega^2)/(\omega^2-f^2) > 0$. There will be IWs.

In this paper, a boundary value problem of second-order linear ordinary differential equations with constant coefficients was transformed into a boundary value problem with variable coefficients. However, it still suffers from the issues related to solving boundary value problems which must be overcome to examine IW features. In this case, the analytical solution cannot be solved, but an approximate method, such as numerical solution, can be used although the theoretical basis of both solutions is the same.

The relationship between sea surface fluctuations and ocean IWs quantified with analytical methods is a prerequisite for reliable retrieval of IWs. It could benefit others interested in understanding the relation of surface and the internal waves through analytical estimation or through numerical modeling of wave characteristics.

References

Alford M H, Peacock T, MacKinnon J A, Nash J D, Buijsman M C,

Centurioni L R, Chao S Y, Chang M H, Farmer D M, Fringer O B, Fu K H, Gallacher P C, Graber H C, Helfrich K R, Jachec S M, Jackson C R, Klymak J M, Ko D S, Jan S, Johnston T M S, Legg S, Lee I H, Lien R C, Mercier M J, Moum J N, Musgrave R, Park J H, Pickering A I, Pinkel R, Rainville L, Ramp S R, Rudnick D L, Sarkar S, Scotti A, Simmons H L, St Laurent L C, Venayagamoorthy S K, Wang Y H, Wang J, Yang Y J, Paluszkiewicz T, (David) Tang T Y (2015). The formation and fate of internal waves in the South China Sea. Nature, 521: 65–69

Alpers W (1985). Theory of radar imaging of internal waves. Nature, 314(6008): 245–247

Brandt P, Romeiser R, Rubino A (1999). On the determination of characteristics of the interior ocean dynamics from radar signatures of internal solitary waves. J Geophys Res Oceans, 104(C12): 30039–30045

Chen B F, Huang Y J, Chen B, Tsai S Y (2016). Surface wave disturbance during internal wave propagation over various types of sea. Ocean Eng, 125: 214–225

Da Silva J C, Buijsman M C, Magalhaes J M (2015). Internal waves on the upstream side of a large sill of the Mascarene Ridge: a comprehensive view of their generation mechanisms and evolution. Deep Sea Res Part I Oceanogr Res Pap, 99: 87–104

Deng B, Zhang M (2006). Spectrum and spectral function analysis of wave in ocean Part I mathematic model and numerical method. Journal of Hydrodynamics (Ser. A), 21(2): 259–266 (in Chinese)

Deng B, Zhang X, Zhang M (2014). Calculation and analysis of vertical structure of internal wave in background current. Advances in Marine Science, 32(2): 121–130 (in Chinese)

Deng B, Zhang Y F, Zhang M (2017). Numerical experiments of oceanic internal wave evolution. Advances in Marine Science, 35(1): 62–72 (in Chinese)

Deng B, Zhang Y F, Zhu J (2016). Theoretical analysis on the stream structure and propagation of unstable ocean internal wave at background shear flow. Marine Forecasts, 33(3): 1–8 (in Chinese)

Fan K G, Fu B, Gu Y Z, Yu X, Liu T, Shi A, Xu K, Gan X (2015). Internal wave parameters retrieval from space-borne SAR image. Front Earth Sci, 9(4): 700–708

Fan K G, Huang W G, Gan X L (2010). Retrieving internal wave surface currents from SAR image. Journal of Remote Sensing, 14(1): 122–130

Fan Z S (2002). Research Fundamentals of Ocean Interior Mixing. Beijing: Maritime Press, 1–3 (in Chinese)

Feng S Z (1999). An Introduction to Marine Science. Beijing: Higher Education Press, 1–4 (in Chinese)

Guo C, Chen X (2014). A review of internal solitary wave dynamics in the northern South China Sea. Prog Oceanogr, 121: 7–23

Li Q (2014). Numerical assessment of factors affecting nonlinear internal waves in the South China Sea. Prog Oceanogr, 121(2): 24–43

Li X, Clemente C P, Friedman K S (2000). Estimating oceanic mixed-layer depth from internal wave evolution from radar sat-1 SAR. Johns Hopkins APL Tech Dig, 21: 130–135

Liu A K, Chang Y S, Hsu M K, Liang N K (1998). Evolution of nonlinear internal waves in the East and South China Seas. J Geophys Res Oceans, 103(C4): 7995–8008

Muacho S, Da Silva J C B, Brotas V, Oliveira P B, Magalhaes J M (2014). Chlorophyll enhancement in the central region of the Bay of Biscay as a result of internal tidal wave interaction. J Mar Syst, 136: 22–30

Porter D L, Thompson D R (1999). Continental shelf parameters inferred from SAR internal wave observation. J Atmos Ocean Technol, 16(4): 475–487

Wei G, Le J C, Dai S Q (2003). Surface effects of internal wave generated by a moving source in a two-layer fluid of finite depth. Appl Math Mech, 24(9): 906–918

Xu Z H, Liu K, Yin B, Zhao Z, Wang Y, Li Q (2016). Long-range propagation and associated variability of internal tides in the South China Sea. J Geophys Res Oceans, 121(11): 8268–8286

Xu Z T (1999). Dynamics of Ocean Internal Wave. Beijing: Science Press, 1−5 (in Chinese)

Yang Q, Zhao W, Liang X, Tian J (2016). Three-dimensional distribution of turbulent mixing in the South China Sea. J Phys Oceanogr, 46(3): 769–788

Yuan Y L, Han L, Qiao F L, Yang Y, Lu M (2011). A unified linear theory of wavelike perturbations under general ocean conditions. Dyn Atmos Oceans, 51(1): 55–74

Zeng K (2002). Three Aspects of Studying Oceanic Internal Wave by Space-Borne Synthetic Aperture Radar Images. Dissertation for Ph.D Degree. Qingdao: Chinese Marine University, 43–58 (in Chinese)

Zhang G R, Zhang J (2009). Ocean Internal Waves and Their Impacts on Naval Warfare. Beijing: China Meteorological Press, 25–29 (in Chinese)

Zhang X, Deng B, Zhang M (2007). Analysis of continuous spectrum wave packet in rotational-stratification two-dimension ocean. Journal of Tropical Oceanography, 26(6): 7–13 (in Chinese)

Zhang X, Deng B, Zhang M (2012). Preliminary study of background current and topography effects on ocean internal wave. Marine Forecasts, 29(3): 26–35 (in Chinese)

Zong J S, Ou Y Y (2011). Ocean Internal Wave Detection with Synthetic Aperture Radar Image. Beijing: Maritime Press, 4–12 (in Chinese)